Infrared Phys. Vol. 29, No. 2-4, pp. 791-798, 1989
Printed in Great Britain

0020-0891/89 $3.00 + 0.00
Pergamon Press plc

FAR INFRARED REFLECTIVITY OF $Tl_2Ba_2CaCu_2O_8$ AND $YBa_2Cu_3O_7$ CERAMICS AND OF AN ORIENTED $YBa_2Cu_3O_7$ THIN FILM

K. F. RENK, W. OSE, T. ZETTERER, J. SCHÜTZMANN, H. LENGFELLNER, H. H. OTTO and J. KELLER
Fakulät Physik, Universität Regensburg, 8400 Regensburg, F.R.G.

and

B. ROAS* and L. SCHULTZ
Siemens AG, Research Laboratories, 8520 Erlangen, F.R.G.

and

G. SAEMANN-ISCHENKO
Physikalisches Institut, Universität Erlangen, 8520 Erlangen, F.R.G.

(*Received 26 September 1988*)

Abstract—We report on measurements of far infrared (IR) reflection spectra of $Tl_2Ba_2CaCu_2O_8$ and $YBa_2Cu_3O_7$ ceramics that are composed of strongly anisotropic crystallites and we present a new method for analyzing reflection spectra of metal–ceramics. In the analysis we take into account that the crystallites have conducting connections. The analysis allows the description of experimental reflection spectra by using Drude's theory of conductivity and introducing appropriate phonon resonances. In a second part we describe results of reflection measurements for an oriented $YBa_2Cu_3O_7$ thin film. We find that the reflectivity above T_c can be described by a Drude-dynamical conductivity for small frequencies ($< 600\,cm^{-1}$) while a strong deviation from a Drude behavior is found for large frequencies. A reflectivity enhancement below T_c gives evidence for a Mattis–Bardeen like conductivity with an energy gap $2\Delta(0)/kT_c \simeq 4.2$.

1. INTRODUCTION

Far infrared reflection studies have been reported for the high-T_c ceramics $La_{2-x}(Ba, Sr)_xCuO_{4-y}$,[1,2] $YBa_2Cu_3O_7$[1-6] and recently also for $Bi_2Sr_2CaCu_2O_8$.[7] The results were analyzed either by homogeneous-medium theories or by an effective-medium theory,[1] in which dielectric functions are mixed in a complicated way; however, these theories were not suitable to deliver satisfactory descriptions of far IR reflection spectra of the conducting ceramics;[5] for a discussion see also Ref. (8). In this paper we report for the first time on a reflectivity measurement for a ceramic $Tl_2Ba_2CaCu_2O_8$ high-T_c superconductor[9] and we present a new method of analysis of far infrared reflection spectra of metal–ceramics. We apply the method to analyze the reflectivity of ceramic $Tl_2Ba_2CaCu_2O_8$ and also of ceramic $YBa_2Cu_3O_7$. We will show that our method leads to a consistent description of reflection spectra of metal–ceramics. In a second part we will describe results of a far IR reflection study of an oriented $YBa_2Cu_3O_7$ film.

2. REFLECTIVITY OF $Tl_2Ba_2CaCu_2O_8$ AND $YBa_2Cu_3O_7$ CERAMIC SAMPLES

Preparation and characterization of ceramic samples are described elsewhere; the $Tl_2Ba_2CaCu_2O_8$ sample[10] had a superconducting transition at $T_c \simeq 105.5\,K$ and the $YBa_2Cu_3O_7$ sample[6] of 86 K.

Far infrared reflection spectra were obtained by use of an IR Fourier spectrometer. By comparing the spectral intensity of radiation reflected from the sample or a gold mirror,

*Also at Physikalisches Institut, Universität Erlangen, 8520 Erlangen, F.R.G.

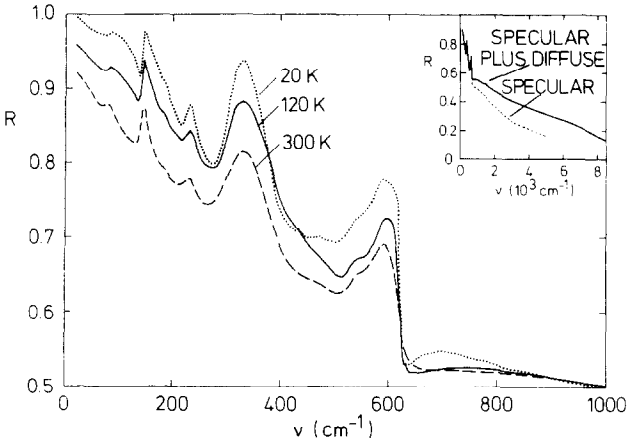

Fig. 1. FIR reflectivity of $Tl_2Ba_2CaCu_2O_8$.

respectively, the reflectivity of the sample was obtained. We measured either specularly reflected radiation or, by collecting radiation in a large solid angle, a sum of specularly and diffusely reflected radiation.[6]

Figure 1 shows the far IR reflectivity of ceramic $Tl_2Ba_2CaCu_2O_8$. The reflectivity drops from a high level at small frequencies to a low level at large frequencies. There is strong structure due to phonons. These appear as minima at small frequencies but as Reststrahlen bands at large frequencies. At low temperature the structure becomes more pronounced, namely reflection minima are sharper and the most prominent Reststrahlen band shows a minimum (near 600 cm^{-1}). It is evident that phonon damping decreases with decreasing temperature. Superconductivity leads finally to an enhancement of reflectivity at small frequencies. For very large frequencies diffuse scattering sets in (inset of Fig. 1). The deviation from specular reflection indicates that the scattering centers have a size of few μm.

Figure 2 shows, for comparison, the far IR reflectivity of ceramic $YBa_2Cu_3O_7$. Again, the reflectivity is high at small frequencies and decreases to a lower value at high frequencies. Phonon structure leads to minima at small frequencies and to a complicated structure at large frequencies. The reflection minima become sharper with decreasing temperature, indicating again less phonon damping at low temperature. Additionally, the spectra show that the size of phonon structure increases strongly with decreasing temperature. Superconductivity is seen by an enhancement of reflectivity for $T < T_c$ at small frequencies and a decrease below the normal state reflectivity at large frequencies.

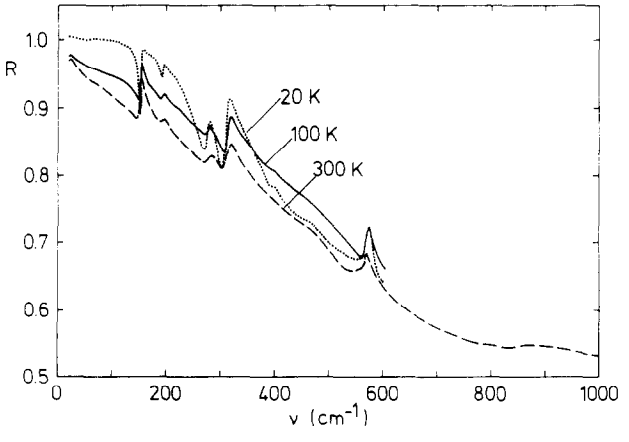

Fig. 2. FIR reflectivity of $YBa_2Cu_3O_7$.

3. ANALYSIS

We relate the form of the far IR spectrum to the geometric structure of the ceramics. Figure 3 shows a scanning electron microscope picture of the surface of our $Tl_2Ba_2CaCu_2O_8$ sample. There are platelets (diameter typically 5 μm) with the crystal c-axis perpendicular to the surface and also platelets with the c-axis in the surface plane (thickness of a platelet along c about 1 μm). Most remarkable are sandwiches of platelets of similar orientation; there are sandwiches with the c-axis almost parallel to the surface. The sandwiches have dimensions of about $5 \times 5 \times 5$ μm or slightly larger. For electromagnetic radiation polarized with the electric field parallel to the c-axis of a sandwich (and supposing that the crystallites are non-conducting along c), the sandwich will appear as dielectric medium embedded in metallic material. The metallic material itself forms a metallic structure. For long-wave radiation this structure will be totally reflecting, while short-wave radiation can penetrate into the dielectric medium.

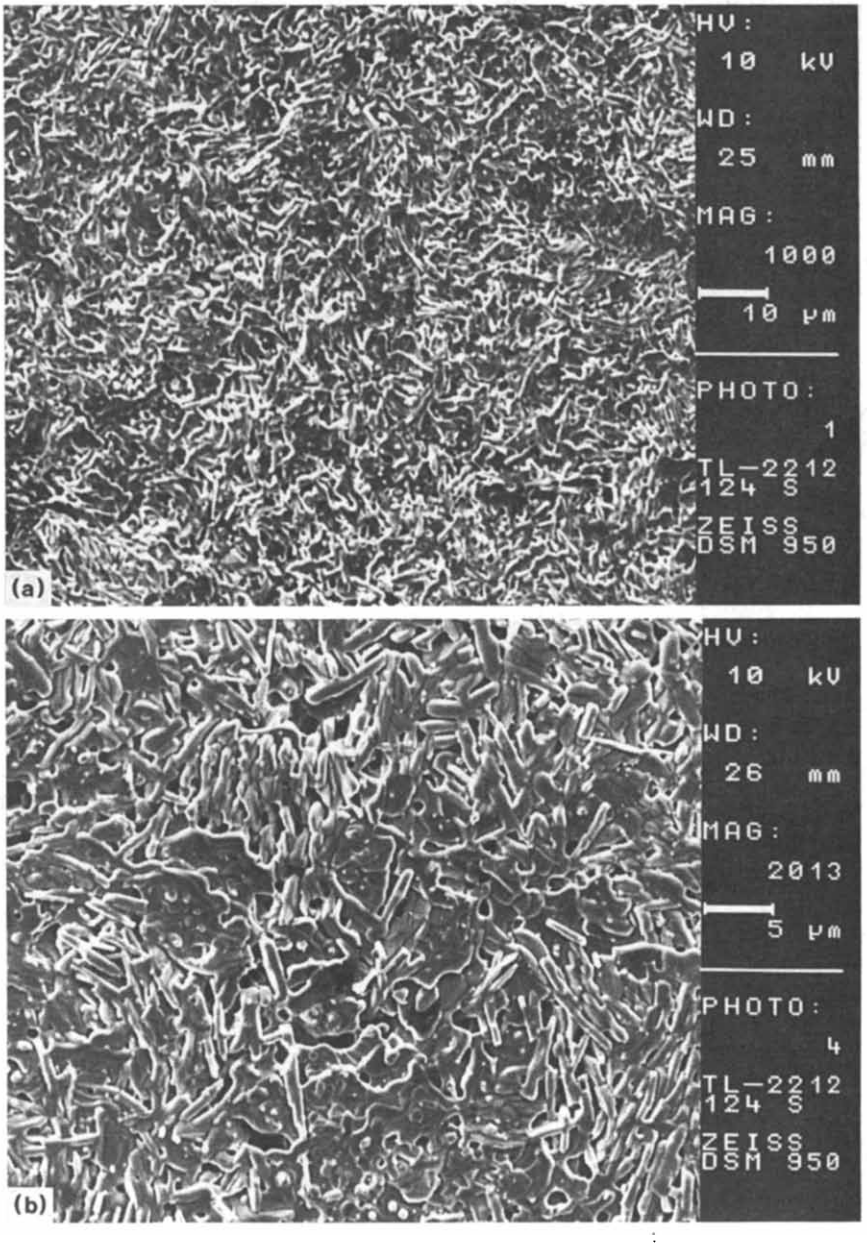

Fig. 3. Scanning electron microscope pictures of our $Tl_2Ba_2CaCu_2O_8$ ceramic sample.

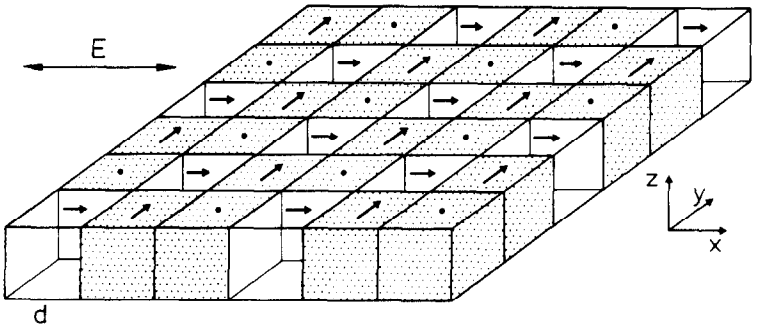

Fig. 4. Model of a metal-ceramics consisting of strongly anisotropic crystallites.

The microscopic picture leads us to a simple model for the ceramics (Fig. 4). We arrange the crystallites (supposed to be cubes) with their c-axis mutually parallel to the x-, y- and z-axis. For an electric field $E \parallel x$ every third crystallite is *dielectric* while the other crystallites are *metallic*; for radiation polarized parallel to the y-axis, a corresponding picture (with other crystallites being dielectric) is obtained. We can describe the structure as a metal plate with rectangular waveguides, filled with dielectric medium. We introduce for the dielectric medium the dielectric function (for $E \parallel c$):

$$\epsilon^{\perp} = \epsilon_{\infty} + \Sigma S_j \nu_j^2 (\nu_j^2 - \nu^2 - i\Gamma_j \nu)^{-1}, \tag{1}$$

where ϵ_{∞} is the high-frequency dielectric constant (which we set $\epsilon_{\infty} = 4$) and where the second term describes phonon resonances (S_j = strength, ν_j = eigenfrequency, Γ_j = damping of the jth mode). We describe propagation in the waveguides by the dielectric function:[11]

$$\epsilon_w = \epsilon^{\perp} - (\lambda/2d)^2, \tag{2}$$

where $\lambda = \nu^{-1}$ is the vacuum wavelength of the radiation and d the width of a waveguide. There is (for the fundamental mode) a cutoff frequency $\nu_c = 1/2n\,d$ where $n^{\perp}$ is a refractive index for $E \parallel c$. For $\nu < \nu_c$ the structure is totally reflecting and for $\nu > \nu_c$ radiation can penetrate into the waveguides. Taking into account phonon resonances, we find that a high-frequency phonon appears as a Reststrahlen-like band and a low-frequency phonon as a reflection minimum [Fig. 5(a)]. The size of the minimum is given by:

$$1 - R \simeq \frac{1}{2}\left(\frac{2d}{\lambda}\right)^3 \epsilon_2^{\perp}, \tag{3}$$

where $\epsilon_2^{\perp}$ is the imaginary part of the dielectric function $\epsilon^{\perp}$ [equation (1)]. Thus we find that the reflection minimum has almost the shape of the phonon resonance curve while the strength of the minimum depends very sensitively on the ratio $2d/\lambda$ and therefore on the dimension of the geometric structure. In Fig. 5(a) it is assumed that two-thirds of incoming radiation intensity is directly reflected at the plane metallic surface and that one-third experiences the waveguide structure. A calculation with more than two phonon resonances and taking into account conduction losses has also been performed [Fig. 5(b)] and leads to a satisfactory agreement with the experiment [Fig. 5(c)]. The analysis delivers a characteristic dimension $d \simeq 8\ \mu$m for the metallic structure that is consistent with the microscopic picture (Fig. 3). We find data for phonon modes summarized in Table 1. The values of S appear to be very reasonable; in a homogeneous-medium theory or an effective-medium theory[1] we had to assume unrealistically large values of the S_j and a strong temperature dependence. The values of Table 1 are given for $T = 120$ K. Changing the temperature leads mainly to a change of the damping constants, but not of the strengths S_j. We attribute the $j = 1$ mode to a Tl vibration (against the rest of the lattice), the $j = 2$ mode to a Ba vibration and the other modes to Cu–O vibrations. We find for the dynamical resistivity (using a Drude conductivity) a value $\rho^{\perp} \simeq 300\ \mu\Omega$ cm (for 100 K) that is comparable to the d.c. resistivity ($\simeq 150\ \mu\Omega$ cm at 100 K). Since the phonon structure is sharp, it follows that the conductivity for $E \parallel c$ is small. We have performed calculations of the reflectivity that give a lower limit of the

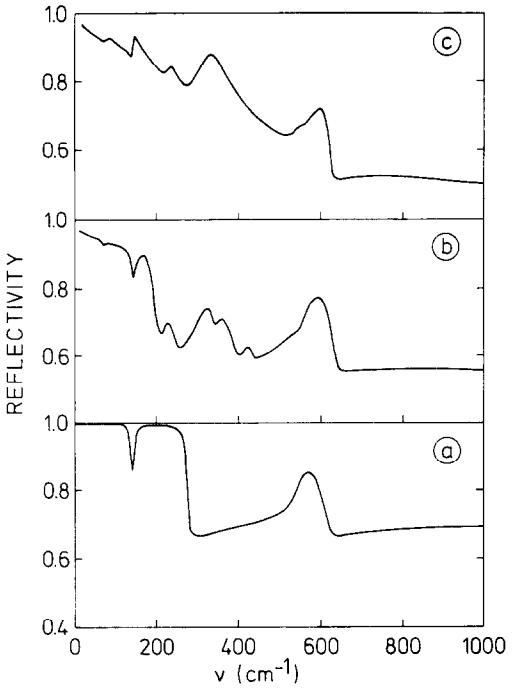

Fig. 5. Calculated reflectivity curves for $Tl_2Ba_2CaCu_2O_8$ (with $d = 8\,\mu m$); (a) for two phonon resonances with $S_1 = S_2 = 0.8$, $\nu_1 = 150\,cm^{-1}$, $\nu_2 = 570\,cm^{-1}$, $\Gamma_1/\nu_1 = \Gamma_2/\nu_2 = 0.05$, $\sigma^{\perp} = \infty$, $\sigma^{\parallel} = 0$; (b) for 8 phonon resonances and finite conductivity $\sigma^{\perp}$; (c) experimental curve (for $T = 120\,K$).

dynamical resistivity $\rho \geqslant 10^3\,\rho^{\perp}$; this may be compared with the anisotropy for $Bi_2Sr_2CaCu_2O_8$,[12] $\rho\,/\rho^{\perp} \simeq 10^5$, and of $YBa_2Cu_3O_7$,[13] $\rho\,/\rho^{\perp} \simeq 100$.

A corresponding analysis for $YBa_2Cu_3O_7$ delivers a characteristic dimension $d \approx 6\,\mu m$, in accordance with electron microscope pictures,[6] and a value for the resistivity (at 100 K) $\rho^{\perp} \approx 300\,\mu\Omega\,cm$, that is comparable to the d.c. value ($\approx 150\,\mu\Omega\,cm$) and $\rho\,/\rho^{\perp} \approx 100$ (at 100 K) in agreement with a d.c. anisotropy measurement.[13] Except the $j = 1$ mode (Table 1) we find the same modes for $YBa_2Cu_3O_7$ as for $Tl_2Ba_2CaCu_2O_8$; the Ba mode is slightly shifted (to $153\,cm^{-1}$) while the other modes appear at almost the same frequencies. The Ba mode is much less damped in $YBa_2Cu_3O_7$ than in $Tl_2Ba_2CaCu_2O_8$. Different *absorption* strengths of the $j = 2$ mode for different $YBa_2Cu_3O_7$ samples[5,6] are most likely due to different characteristic dimensions d leading to different values for $1 - R$ according to equation (3).

A comparison of different barium cuprates ($YBa_2Cu_3O_7$, $YBa_2Cu_3O_6$, Y_2BaCuO_5,[15] $Tl_2Ba_2CuO_6$, $Tl_2Ba_2CaCu_2O_8$) indicates that these have in common a Ba vibration with a strength $S \approx 0.8$ (with an eigenfrequency between 110 and $153\,cm^{-1}$), a high-frequency Cu–O vibration with $S \approx 0.8$ (near $570\,cm^{-1}$) and a low frequency Cu–O vibration with $S \approx 1$; this prominent mode has an eigenfrequency (between 300 and $340\,cm^{-1}$) that is different for different barium cuprates and is temperature dependent.

Table 1. Phonons in $Tl_2Ba_2CaCu_2O_8$ (at 120 K)

j	$\nu_j\,(cm^{-1})$	S_j	$\Gamma_j\,(cm^{-1})$
1	71	0.8	10
2	142	0.8	10
3	221	0.4	30
4	311	1	30
5	350	0.4	40
6	420	0.2	40
7	540	0.4	40
8	565	0.5	20
	ΣS_j	4.5	

We note that we had to consider reflection of radiation from lower sheets of the surface. This is expected for frequencies above the two-phonon cutoff-frequency (at 1200 cm^{-1}).[6] Then, the dielectric regions (for a given polarization) are transparent and reflection from metallic platelets below dielectric platelets add to the reflectivity of the outer surface. This may lead to enhanced reflectivity discussed earlier[8,16] that has been attributed to an excitonic excitation.[16]

4. REFLECTIVITY OF AN ORIENTED $YBa_2Cu_3O_7$ THIN FILM

Our film (thickness about 4000 Å), on a $SrTiO_3$ substrate, has been prepared by a laser evaporation technique;[17,18] the d.c. resistivity was about 60 $\mu\Omega$ cm at 100 K and increased almost linearly with temperature. The film had a sharp transition at $T_c = 91$ K; the critical current was $2 \cdot 10^6$ A cm^{-2} at 77 K.

Experimental results of reflection measurements are drawn in Fig. 6(a). At high temperature ($T > T_c$), the reflectivity curves have similar shape. For $T < T_c$ the shape has changed; the reflectivity is almost 1 up to a frequency of 150 cm^{-1} and decreases towards large frequencies, and is for $\nu \geqslant 600$ cm^{-1} slightly smaller than the reflectivity for the normal state at 100 K. In Fig. 6(b) we have plotted the ratio of the reflectivity at 20 K and the reflectivity at 100 K. The ratio increases (from 1) at small frequencies, reaches a maximum near 300 cm^{-1}, then decreases, and becomes 1 near 600 cm^{-1}.

Figure 7 shows the reflectivity at larger frequencies. The reflectivity at 100 K remains over the whole frequency range of our experiment slightly larger than the reflectivity at 300 K.

For an analysis of the reflectivity for $T > T_c$ we use the Drude conductivity $\sigma = \sigma_0(1 - i\nu/\nu_\tau)^{-1}$ where σ_0 is the dynamical conductivity for $\nu \ll \nu_\tau$ and ν_τ the scattering rate of the charge carriers; we have taken into account reflection losses of the gold mirror ($\rho \simeq 1$ $\mu\Omega$ cm) for room temperature, while we assumed $R \simeq 1.00$ for $T \leqslant T_c$. At small frequencies the absorptivity can be described in the Hagen–Rubens approximation $1 - R \simeq (16\pi\epsilon_0 c\nu/\sigma_0)^{1/2}$ where ν is the frequency (divided by the velocity of light, c) and $\epsilon_0 = 8.9 \cdot 10^{-12}$ $AsV^{-1}m^{-1}$. We obtain calculated curves [solid lines of Fig. 6(a)] that describe the experimental data reasonably well, with values for the dynamical resistivity σ_0^{-1} drawn in the inset of Fig. 7. We find that the dynamical resistivity is almost equal to the d.c. resistivity, showing a linear temperature dependence. For large frequencies the reflectivity curves show a strong deviation from a Drude behavior. Taking for $T = 300$ K a scattering rate $\nu_\tau \approx 2700$ cm^{-1}, corresponding to a scattering time $\tau = (2\pi c\nu_\tau)^{-1} \approx 2 \times 10^{-15}$ s, and for 300 K ν_τ (300 K) $\approx \nu_\tau$(100 K) we find the solid lines of Fig. 7. The experimental reflectivity curves lie below the calculated curves, indicating that the reflectivity is not Drude like for large frequencies. The reason for this behavior is not yet known.

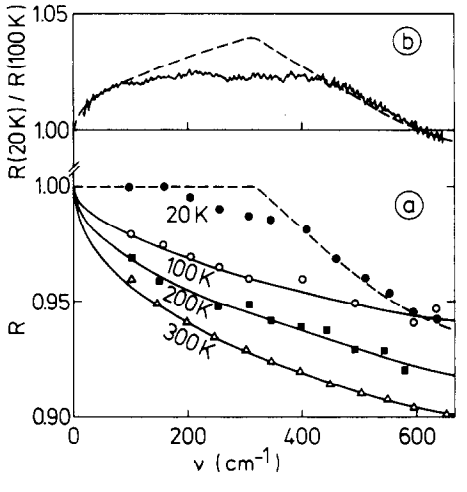

Fig. 6. FIR reflectivity of an oriented $YBa_2Cu_3O_7$ film (a) and reflectivity ratio (b).

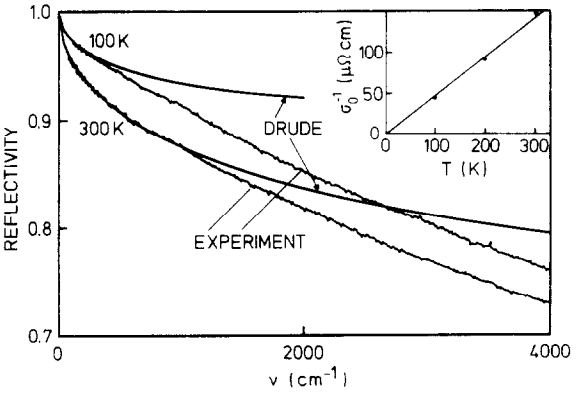

Fig. 7. Reflectivity of the oriented $YBa_2Cu_3O_7$ thin film in the IR; inset, dynamical resistivity.

For a further discussion of our results we apply, for simplicity, a model of a 2-D free electron gas. Taking account of the crystal structure and the lattice parameters ($a \simeq 3.8$ Å, $b \simeq 3.9$ Å, $c \simeq 11.67$ Å), we find from the resistivity σ_0^{-1} ($\approx 50\,\mu\Omega$ cm, inset of Fig. 6) a 2-D conductivity $\Sigma_0 \approx 1.1 \times 10^{-3}\,\Omega^{-1}$ (for 100 K). Using the relation[19] $\Sigma_0 = \frac{1}{2}e^2\tau v_F^2 n(E_F)$ where v_F is the Fermi velocity of the charge carriers and $n(E_F)$ the 2-D density of states at the Fermi energy, E_F, we obtain for the product $v_F^2 n(E_F) \approx 4.3 \times 10^{49}\,J^{-1}\,s^{-2}$. Taking for the density of states $n(E_F) = m/\pi\hbar^2$ and for m the value of the free electron mass we find $v_F \approx 1.2 \times 10^6\,ms^{-1}$ and a Fermi wave vector $k_F = v_F m/\hbar \approx 1.1 \times 10^{10}\,m^{-1}$. From the Fermi wave vector we find a concentration $n = k_F^2/2\pi \approx 1.9 \times 10^{19}\,m^{-2}$ that is not much different from a value ($1.4 \times 10^{19}\,m^{-2}$) obtained if it is assumed that four free holes per unit cell are contained in the Cu–O planes. Our analysis leads to a m.f.p. $l = v_F\tau \approx 24$ Å (at 100 K). Supposing that $n(E_F)$ is independent of temperature our results are consistently explained with a m.f.p. that varies as T^{-1}. This can be explained by a scattering of charge carriers at acoustic phonons.[19]

From the Sommerfeld parameter γ derived from the jump of the specific heat at T_c[20] and from a magnetic study[21] a density of states of the Fermi energy two or three times as large as derived by our analysis is obtained; this is, in view of our simple model, a satisfactory agreement. The m.f.p. l we found corresponds almost to the coherence length ξ_0 in the superconducting state;[21,22] this is expected for a "dirty" superconductor.

For a discussion of the reflectivity in the superconducting state we use the theory of Mattis and Bardeen.[23] A description of our results using a gap frequency $\nu_g \simeq 300\,cm^{-1}$ appears to be reasonable (Fig. 5; dashed curves follow from theory). However, there is a clear discrepancy between theory and experiment, namely the reflectivity does not reach a value of 1 at frequencies directly below the assumed gap frequency. This deviation may be caused by imperfectness of the film; it seems also possible that there are excitation states for $\nu < \nu_g$. Our assumed gap energy of $2\Delta(0)/kT_c \simeq 4.2$ corresponds to values of strong coupling superconductors. We note that this value is in the middle of values (2 to 8) obtained from studies of ceramic samples,[1–6] films,[24,25] and for mosaic crystals.[26]

5. CONCLUSION

We have presented an experimental study of the reflectivity of ceramic $Tl_2Ba_2CaCu_2O_8$ and $YBa_2Cu_3O_7$ samples. We have applied a new method for analyzing reflection spectra of metal–ceramic that allowed determination of characteristic properties of phonons and charge carriers. In our analysis we have taken into account that a metal–ceramic consisting of crystallites with strongly anisotropic conductivity appears for a given polarization vector of the electromagnetic radiation as a metal plate containing holes filled with material oriented with $c \parallel E$; long-wave radiation is almost totally reflected at the structure while short-wave radiation can propagate into the holes; this model allows us to explain that a low-frequency IR-active phonon mode appears as narrow reflection minimum while a high-frequency mode can give rise to a Reststrahlen band. Our analysis leads to a satisfactory description of phonons and also of free charge carriers; for these we find Drude-like behavior (for temperatures above T_c). In a second part of the paper we reported on properties of oriented $YBa_2Cu_3O_7$ thin films. The reflectivity above T_c can be described by Drude's theory of conductivity for a 2-D electron gas in the range of small frequencies ($\nu \leqslant 600\,cm^{-1}$). There are, however, strong deviations from Drude's theory at large frequencies, namely the experimental conductivity is much smaller than expected from the Drude theory. The reason for this behavior is not yet clear. Evidence for an energy $2\Delta(0)/kT_c \approx 4.2$ is found.

Acknowledgement—The work was supported by the Bundesministerium für Forschung und Technologie.

REFERENCES

1. T. W. Noh, P. E. Sulewski and A. J. Sievers, *Phys. Rev.* **B36,** 8866 (1987).
2. Z. Schlesinger, R. T. Collins, W. M. Shafer and E. M. Engler, *Phys. Rev.* **B36,** 5275 (1987).
3. G. A. Thomas, H. K. Ng, A. J. Millis, R. N. Bhatt, R. J. Cava, E. A. Rietman, D. W. Johnson Jr, G. P. Epinosa and J. M. Vanderberg, *Phys. Rev.* **B46,** 846 (1987).
4. L. Genzel, A. Wittlin, A. Kuhl, Hj. Mattausch, W. Bauhofer and A. Simon, *Solid State Commun.* **63,** 843 (1987).

5. T. Timusk, D. A. Bonn, J. E. Breedan, C. V. Stager, J. D. Garrett, A. H. O'Reilly and M. Reedyk, *Physica C* **1253–155,** 1744 (1988).
6. W. Ose, P. E. Obermayer, H. H. Otto, T. Zetterer, H. Lengfellner, J. Keller and K. F. Renk, *Z. Phys. B—Condensed Matter* **70,** 307 (1988).
7. Z. V. Popovic, C. Thomsen, M. Cardona, R. Lin, S. Stanisic, R. Kremer and W. Knig, *Solid State Commun.* **66,** 965 (1988).
8. J. Orenstein and D. H. Rapkine, *Phys. Rev. Lett.* **60,** 968 (1988); K. Kamarás, C. D. Porter, M. G. Doss, S. L. Herr, D. B. Tanner, D. A. Bonn, J. E. Greedan, A. H. O'Reilly, C. V. Stager and T. Timusk, *Phys. Rev. Lett.* **60,** 969 (1988).
9. Z. Z. Sheng and A. M. Hermann, *Nature* **332,** 55 (1988); *ibid.* **332,** 138 (1988).
10. T. Zetterer, H. H. Otto, G. Lugert and K. F. Renk, *Z. Phys. B.* **73,** 321 (1988).
11. F. Keilmann, *Int. J. Infrared & Millimeter Waves* **2,** 259 (1981).
12. S. W. Tozer, A. W. Kleinsasser, T. Penney, D. Kaiser and F. Holtzberg, *Phys. Rev. Lett.* **59,** 1768 (1987).
13. S. Martin, A. T. Fiory, R. M. Fleming, L. F. Schneemeyer and J. V. Waszczak, *Phys. Rev. Letlt.* **60,** 2164 (1988).
14. R. Liu, C. Thomsen, W. Kress, M. Cardona, B. Gegenheimer, F. W. de Wette, J. Prade, A. D. Kulkarnis and U. Schröder, *Phys. Rev.* **B37,** 7971 (1988).
15. K. F. Renk, H. Lengfellner, P. E. Obermayer, W. Ose, H. H. Otto and T. Zetterer, *Int. J. Infrared & Millimeter Waves* **8,** 1525 (1987).
16. K. Kamarás, C. D. Porter, M. G. Doss, S. L. Herr, D. B. Tanner, D. A. Bonn, J. E. Greedan, A. H. O'Reilly, C. V. Stager and T. Timusk, *Phys. Rev. Lett.* **59,** 919 (1987).
17. B. Roas, L. Schultz and W. Kautek, *DVS Report*, Vol. **113.** DVS Verlag, Düsseldorf (1988).
18. B. Roas, G. Endres and L. Schultz, *Appl. Phys. Lett.* October 24 (1988).
19. J. M. Ziman, *Principles of the Theory of Solids.* Cambridge University Press (1979).
20. S. E. Inderhees, M. B. Salamon, N. Goldenfeld, J. P. Rice, B. G. Pazol, D. M. Ginsberg, J. Z. Liu and G. W. Crabtree, *Phys. Rev. Lett.* **60,** 1178 (1988).
21. R. J. Cava, B. Batlogg, R. B. van Dover, D. W. Murphy, S. Sunshine, T. Siegrist, J. P. Remeika, E. A. Rietmann, S. Zahurak and G. P. Espinosa, *Phys. Rev. Lett.* **58,** 1676 (1987).
22. A. Kapitulnik, *Physica C* **153–155,** 520 (1988).
23. D. C. Mattis and J. Bardeen, *Phys. Rev.* **111,** 412 (1958).
24. G. A. Thomas, R. N. Bhatt, A. Millis, R. Cava and E. Rietman, *Jap. J. Appl. Phys.* **26,** 1001 (1987).
25. R. T. Collins, Z. Schlesinger, R. H. Koch, R. B. Laibowitz, T. S. Plaskett, P. Freitas, W. J. Gallagher, R. L. Sandstrom and T. R. Dinger, *Phys. Rev. Lett.* **59,** 704 (1987).
26. Z. Schlesinger, R. T. Collins, D. L. Kaiser and F. Holtzberrg, *Phys. Rev. Lett.* **59,** 1958 (1987).